Mitochondrial gene in the nuclear genome induces reproductive barrier in rice

Yoshiyuki Yamagata[a], Eiji Yamamoto[b], Kohichiro Aya[b], Khin Thanda Win[a], Kazuyuki Doi[a,1], Sobrizal[a,2], Tomoko Ito[c], Hiroyuki Kanamori[c], Jianzhong Wu[d], Takashi Matsumoto[d], Makoto Matsuoka[b], Motoyuki Ashikari[b], and Atsushi Yoshimura[a,3]

[a]Faculty of Agriculture, Kyushu University, Hakozaki, Higashi, Fukuoka 812-8581, Japan; [b]Bioscience and Biotechnology Center, Nagoya University, Furo, Chikusa, Nagoya, Aichi 464-8601, Japan; [c]Institute of the Society for Techno-innovation of Agriculture, Forestry and Fisheries, Kamiyokoba, Tsukuba, Ibaraki 305-0854, Japan; and [d]Division of Genome and Biodiversity Research, National Institute of Agrobiological Sciences, Kannondai, Tsukuba, Ibaraki 305-8602, Japan

Edited by Gurdev S. Khush, University of California, Davis, CA, and approved November 25, 2009 (received for review July 28, 2009)

Hybrid incompatibility in F_1 hybrids or later generations is often observed as sterility or inviability. This incompatibility acts as post-zygotic reproductive isolation, which results in the irreversible divergence of species. Here, we show that the reciprocal loss of duplicated genes encoding mitochondrial ribosomal protein L27 causes hybrid pollen sterility in F_1 hybrids of the cultivated rice *Oryza sativa* and its wild relative *O. glumaepatula*. Functional analysis revealed that this gene is essential for the later stage of pollen development, and distribution analysis suggests that the gene duplication occurred before the divergence of the AA genome species. On the basis of these results, we discuss the possible contribution of the "founder effect" in establishing this reproductive barrier.

F_1 pollen sterility | gene duplication | BDM incompatibility | mitochondrial ribosomal protein

In *On the Origin of Species*, Darwin argued the importance of natural selection in the evolution of species (1). Through natural selection, mutations increasing fitness will become fixed in a population, whereas those reducing fitness will be removed. The sterility and inviability observed in hybrids between two species are obvious traits that decrease fitness. Therefore, the existence of these traits has been pointed out as a contradiction of natural selection. Bateson, Dobzhansky, and Muller explained this contradiction using a genetic model in which hybrid sterility and inviability are caused by sets of interacting "complementary genes" (2, 3). This model is widely accepted and called the Bateson–Dobzhansky–Muller (BDM) incompatibility model. A molecular study of *Drosophila* revealed that the interaction of protein products from multiloci (4–7) and gene transposition (8) could lead the BDM incompatibility in hybrids. In plants, hybrid incompatibility conferring inviability, sterility, and necrosis (or weakness) in the F_1 and F_2 generation has been frequently found (9–11). Epistatic interaction between dominant or recessive alleles at multiple loci triggers zygotic (or sporophytic) BDM incompatibility in hybrids in various species. Recent gene cloning studies contribute to an understanding of the mechanism of the epsitatic interaction between the loci in plants (12, 13). One study of "hybrid necrosis," one of the reproductive barriers widely distributed in plant species (11), demonstrated that one dominant allele encoding nucleotide binding site–leucine-rich repeat (NBS-LRR) genes causes characteristic autoimmune reactions in F_1, which are similar to phenotypes associated with response to environmental stress, such as pathogen attack in *Arabidopsis thaliana* (12). Another recent study demonstrated that interaction of recessive alleles between two loci, which emerged from gene duplication and its reciprocal loss in each diverged population, cause hybrid inviability in the F_2 generation in *A. thaliana* (13). On the other hand, cloning of the gene for gametic (or gametophytic) BDM incompatibility is limited, except as cited in one seminal work for the *Sa* locus identified in an inter-subspecific cross in rice (14). The *Sa* locus had been recognized as a single Mendelian factor, but this locus contained two adjacent genes interacting with each other, and divergence of the genes in each subspecies caused gametophytic pollen sterility in their hybrid.

In rice, pollen sterility in F_1 hybrids is a major reproductive isolation barrier between cultivated rice *Oryza sativa* and its wild relatives (15, 16). To explain the genetic mechanism of such F_1 sterility, two models have been proposed according to the mode of Menderian inheritance: the one-locus allelic interaction and the two-locus epistatic interaction (16). Recently, two cases of the gametophytic F_1 pollen and embryo sac sterility fitting the one-locus allelic interaction model were analyzed at the molecular level (14, 17). However, the molecular mechanism of gametophytic F_1 sterility fitting the two-locus model could not be understood although the possible cause of sterility was estimated to be due to duplicated genes, which are essential for gamete development in the classic genetic analysis in rice (18).

In this study, we demonstrated that reciprocal loss of duplicated genes causes hybrid sterility in F_1 between *O. sativa* and *O. glumaepatula*. These genes encode mitochondrial ribosomal protein L27, which is essential for the late developmental stage of pollen. Furthermore, we analyzed the distribution of the duplicated locus in the rice AA genome species, and its evolutional trajectory was discussed.

Results

Epistatic Interaction Between *S27* and *S28*. *O. glumaepatula* is a wild rice distributed in the Amazon basin (19). The F_1 hybrid between the cultivated variety Taichung 65 [*O. sativa* ssp. *japonica* (T65)] and the *O. glumaepatula* accession IRGC105668 exhibits complete pollen sterility (Fig. 1 *A* and *B*), but its pistils can accept fertile pollen and produce mature seeds. On the basis of these

Author contributions: Y.Y., M.A., and A.Y. designed research; Y.Y., E.Y., K.A., K.T.W., and K.D. performed research; S. and A.Y. developed the plant materials; T.I., H.K., J.W., and T. M. undertook the BAC clone analysis; M.M. provided advice on the experiments and writing; and Y.Y. and A.Y. wrote the paper.

The authors declare no conflict of interest.

This article is a PNAS Direct Submission.

Date deposition: The sequences reported in this paper have been deposited in the DNA Data Base in Japan [accession nos. AB496673 (*mtRPL27a S27-T65*$^+$), AB496674 (*mtRPL27b S27-T65*$^+$), and AB496675 (*mtRPL27a S28-glum*$^+$)].

[1]Present address: Graduate School of Bioagricultural Sciences, Nagoya University, Furo, Chikusa, Nagoya, Aichi 464-8601, Japan.

[2]Present address: National Nuclear Energy Agency, Center for the Application of Isotopes and Radiation Technology, Jalan Lebak Bulus Raya, P.O. Box 7002, JKSL, Jakarta 12070, Indonesia.

[3]To whom correspondence should be addressed at: Faculty of Agriculture, Kyushu University, 6-10-1 Hakozaki, Higashi, Fukuoka 812-8581, Japan. E-mail: ayoshi@agr.kyushu-u.ac.jp.

This article contains supporting information online at www.pnas.org/cgi/content/full/0908283107/DCSupplemental.

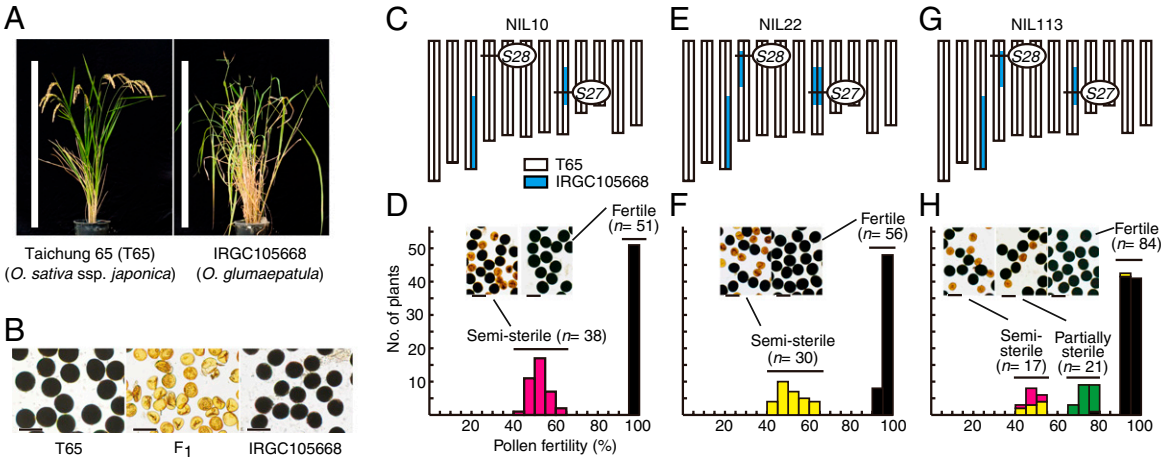

I

Genotype of pollen grain			Fertility
S27-T65$^+$	*S28-T65*^{s}	(T^+|T^s)	Fertile
S27-T65$^+$	*S28-glum*$^+$	(T^+|G^+)	Fertile
S27-glum^s	*S28-T65*^{s}	(G^s|T^s)	Sterile
S27-glum^s	*S28-glum*$^+$	(G^s|G^+)	Fertile

J

Genotype of plant (*S27*/*S27* | *S28*/*S28*)	Genotype of pollen grain T^+|T^s	T^+|G^+	G^s|T^s	G^s|G^+	Expected pollen fertility	Expected segregation ratio
T^+/T^+ | T^s/T^s	●	–	–	–	100%	1
T^+/T^+ | T^s/G^+	●	●	–	–	100%	2
T^+/T^+ | G^+/G^+	–	●	–	–	100%	1
T^+/G^s | T^s/T^s	●	–	●	–	50%	1
T^+/G^s | T^s/G^+	●	●	●	●	75%	3
T^+/G^s | G^+/G^+	–	●	–	●	100%	2
G^s/G^s | T^s/T^s	–	–	●	–	0%	0
G^s/G^s | T^s/G^+	–	–	●	●	50%	1
G^s/G^s | G^+/G^+	–	–	–	●	100%	1

Fig. 1. Epistasis between *S27* and *S28*. (*A*) T65 and IRGC105668 plants. Scale bars: 1 m. (*B*) I_2–KI-stained pollen of T65, IRGC105668, and their F_1 hybrid. Scale bars: 50 μm. (C and D) Genetic analysis of *S27* using NIL10. (*E* and *F*) Genetic analysis of *S28* using NIL22. (*G* and *H*) Genetic analysis of the epistatic interaction between *S27* and *S28* using NIL113. (*C*, *E*, and *G*) The graphical genotypes of the NILs. (*D*, *F*, and *H*) Frequency distribution of pollen fertility in the progeny of each NIL. Pink, yellow, green, and black in the histograms indicate the genotypes of individuals represented in *J*. (*I*) Gametophytic epistatic model of hybrid pollen sterility. (*J*) Expected classes of genotypes and pollen fertility in self-pollinated progeny of plants heterozygous at both *S27* and *S28*.

characteristics, we developed near-isogenic lines (NILs) by pollinating the F_1 hybrids with T65 pollen. Genetic studies using these NILs revealed that the F_1 pollen sterility is controlled by several loci, including *S27* and *S28* (20–23). On the basis of a genetic analysis of three NILs (Fig. 1 *C*, *E*, and *G*) using two tightly linked markers, *S27_ssr1* for *S27* and *S28_10* for *S28*, we found an epistatic interaction between *S27* on chromosome 8 and *S28* on chromosome 4.

In the self-pollinated progeny of NIL10 (*S27* heterozygous and *S28-T65* homozygous) (Fig. 1*C*), *S27* heterozygotes were semisterile and *S27-T65* homozygotes were completely fertile, and no *S27-glum* homozygote was obtained (Fig. 1*D*). This result indicates that the *S27-glum* allele causes pollen sterility in this genetic background. In the self-pollinated progeny of NIL22 (*S27-glum* homozygous and *S28* heterozygous) (Fig. 1*E*), *S28* heterozygotes were semisterile and *S28-glum* homozygotes were completely fertile, and no *S28-T65* homozygote was obtained (Fig. 1*F*). Again, this indicates that the *S28-T65* allele causes pollen sterility in this genetic background. Taken together, we hypothesized that *S27* and *S28* interact epistatically in a gametophytic manner and that pollen grains carrying *S27-glum* and *S28-T65* would be sterile.

To confirm this hypothesis, the self-pollinated progeny of NIL113 (*S27* and *S28* heterozygous) were tested (Fig. 1 *G* and *H*). According to the hypothesis, the fertility of a single pollen grain is determined by the genotype of the pollen grain at the *S27* and *S28* loci (Fig. 1*I*); *i.e.*, *S27-glum* and *S28-T65* alleles are sterile, whereas *S27-T65* and *S28-glum* are fertile alleles (hereafter, sterile alleles are indicated by a superscript *s* and fertile ones by a superscript "+"). Consequently, pollen grains carrying a set of sterile alleles, *S27-glum*^{s} and *S28-T65*^{s}, should be sterile whereas pollen grains carrying at least one fertile allele, *S27-T65*$^+$ or *S28-glum*$^+$, should be fertile (Fig. 1*I*). In this context, the pollen fertility of plants heterozygous at both the *S27* and *S28* loci should become 75%, and self-pollinated plants will show 100%, 75%, and 50% pollen fertility with a segregation ratio of 7:3:2, respectively (Fig. 1*J*). Indeed, the progeny of NIL113 were divided into three classes (Fig. 1*H*): semisterile, partially sterile, and fertile with an average pollen fertility of 48.9%, 74.1%, and 94.8%, respectively, and the segregation of pollen fertility in the progeny fit our hypothesis (Table S1). Spikelet fertility of each pollen fertility class was normal, indicating that *S27* and *S28* did not affect female gamete fertility.

Map-Based Cloning. We performed map-based cloning of *S27* and *S28*. High-resolution mapping revealed that *S27* and *S28* are located in 134.9-kb and 1.68-Mb regions on chromosomes 8 and 4, respectively (Fig. S1). Ueda et al. (24) reported ≈30-kb duplicated segments in our candidate regions for *S27* and *S28* in the Nipponbare genome (Fig. S1, yellow boxes). Therefore, we determined the sequences around these duplicated segments of T65 and *O. glumaepatula* and found similar duplicated segments in the *S27-T65*$^+$, *S28-T65*^{s}, and *S28-glum*$^+$ alleles, but not in the *S27-glum*^{s} allele (Fig. 2*A*, arrow). We speculated that genes located in these duplicated segments are associated with the epistatic interaction between *S27* and *S28*, whereas *S27-glum*^{s} may be a loss-of-function allele due to the absence of the duplicated segment. The gene prediction by the Rice Genome Automated Annotation System (25) suggested that the corresponding region of *S27-T65*$^+$ contains the UDP-glycosyltransferase gene (*UDPGT*) and two tandem

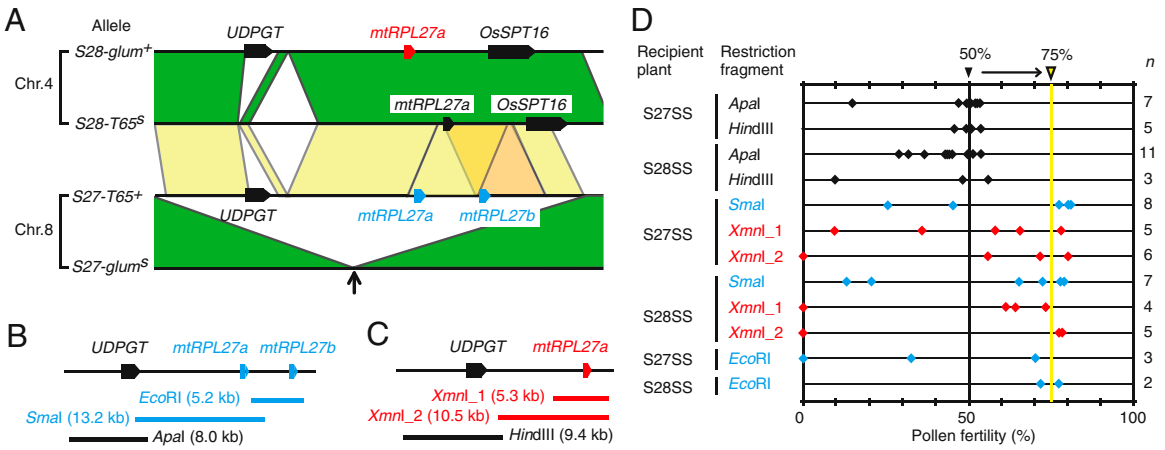

Fig. 2. Map-based cloning of *S27* and *S28*. (*A*) The genomic sequences of T65 and *O. glumaepatula* in the duplicated segments at *S27* and *S28*. The conserved genomic regions between homologous chromosomes and between nonhomologous chromosomes are connected with green and yellow, respectively. The tandem genomic duplicate containing *mtRPL27b* in the *S27-T65*$^+$ allele is indicated by orange. Pentagons represent the predicted genes. The segmental duplicated segments did not exist in *S27-glum*^{s} allele (arrow). (*B* and *C*) Locations of the restriction fragments of *S27-T65*$^+$ (*B*) and *S28-glum*$^+$ (*C*) used in the complementation test. (*D*) Pollen fertility of T_0 plants transformed with the restriction fragments in *B* and *C*. *S27*SS and *S28*SS represent the *S27* semisterile and *S28* semisterile plants, respectively (see text for their genotypes). The expected pollen fertility of the recipient plants is 50%. The rescued plants are expected to show 75% pollen fertility.

mitochondrial ribosomal protein L27 genes (*mtRPL27a* and *mtRPL27b*), whose amino acid sequences are identical (Fig. 2*A* and Fig. S2). In the *S28* region, one *UDPGT* and one *mtRPL27* are predicted in *S28-glum*$^+$, and one *mtRPL27* and no *UDPGT* are predicted in *S28-T65*^{s}. On the basis of the genomic sequence similarity, including the promoter region of the genes, the *mtRPL27* genes predicted in *S28-T65*^{s} and *S28-glum*$^+$ appeared to correspond to *mtRPL27a* in *S27-T65*$^+$. The *S28-T65*^{s} and *S28-glum*$^+$ regions also contain another gene (*OsSPT16*), which encodes a homolog of yeast *spt16* (24) and is not seen in the *S27-T65*$^+$ region (Fig. 2*A*).

Next, we transformed the genomic fragments containing various genome sequences derived from the fertile alleles *S27-T65*$^+$ and *S28-glum*$^+$ (Fig. 2 *B* and *C*) into the pollen-semisterile plants carrying *S27-T65*$^+$/*S27-glum*^{s}|*S28-T65*^{s}/*S28-T65*^{s} (*S27* semisterile plants) or plants carrying *S27-glum*^{s}/*S27-glum*^{s}|*S28-T65*^{s}/*S28-glum*$^+$ (*S28* semisterile plants). Theoretically, when the transformed genomic fragment has the ability to rescue pollen sterility and is introduced at one locus of the host plants, pollen fertility is rescued from 50% to 75% in T_0 plants (the rightmost line in Fig. 2*D*). When the genomic fragment containing *mtRPL27a* (the *Sma*I fragment from T65 in Fig. 2*B* and the *Xmn*I_1 or *Xmn*I_2 fragment from *O. glumaepatula* in Fig. 2*C*) or *mtRPL27b* (the *Eco*RI fragment in Fig. 2*B*) was transformed, transgenic plants exhibited ≈75% pollen fertility, whereas the introduction of *UDPGT* (the *Apa*I fragment in Fig. 2*B* or the *Hin*dIII fragment in Fig. 2*C*) did not affect pollen fertility (Fig. 2*D*). These results demonstrate that the duplicated genes encoding the mtRPL27 protein at *S27* and *S28* are involved in this pollen sterility, whereas *mtRPL27a* on *S28-T65*^{s} is a loss-of-function allele caused by failure of expression (see below).

Mechanism of Pollen Sterility. To unravel the mechanism of pollen sterility, we observed the pollen of *S28* semisterile plants at each developmental stage (Fig. 3*A*). No phenotypic abnormality was observed at the tetrad or unicellular stages (Fig. S3). At the late bicellular stage, we detected generative and vegetative cells in all pollen grains (Fig. 3 *C* and *D*), but half of them failed to initiate starch accumulation (Fig. 3*B*). At the mature stage, two sperm cells and one vegetative cell were detected in half of the pollen grains (Fig. 3*F*), and the remainder were still arrested at the bicellular stage without starch accumulation (Fig. 3 *E* and *G*). Furthermore, because the causal genes of *S27* and *S28* encode mtRPL27 protein, which is localized in mitochondria (24), we observed mitochondria in pollen grains at the mature stage using transmission electron microscopy (Fig. 3 *H* and *I*). In the mitochondria of the fertile pollen, a developed matrix structure and intermembrane space were observed (Fig. 3*H*), whereas no such complex structure was observed in the mitochondria of sterile pollen grains (Fig. 3*I*). In bacteria, ribosomes lacking RPL27 protein are defective in protein synthesis (26). This suggests that a defect of mtRPL27 inhibits protein synthesis in mitochondria, and consequently its respiratory activity is defective and it produces sterile pollen.

An expression analysis of *mtRPL27* was performed. Transcription of *mtRPL27* was observed in various plant tissues, including leaf, leaf sheath, root, and flower (Fig. S4). The expression of *mtRPL27* in anther during pollen development was analyzed by quantitative RT–PCR (Fig. S4). About twofold greater expression was observed in the bicellular and mature stages relative to the unicellular stage. This matches the microscopic observations and supports the importance of the mtRPL27 protein for pollen development from the bicellular to the mature stage.

Next, we examined the expression of *mtRPL27a* at *S28-T65*^{s} in T65. Although several amino acid substitutions were observed (Fig. S2), we speculated that the loss-of-function at *S28-T65*^{S} is caused by failure of expression because a loss of promoter activity of *mtRPL27* at this locus has been reported in Nipponbare (24), a close relative of T65. When we analyzed the DNA sequence of the RT–PCR products from T65 anthers, we detected only the *mtRPL27a* or *mtRPL27b* sequence of *S27-T65*$^+$, and not *mtRPL27a* of *S28-T65*^{s}, which suggests that *mtRPL27a* at the *S28-T65*^{s} locus is not transcribed. Furthermore, we confirmed the loss of expression of *S28-T65*^{s} by using allele-specific semiquantitative RT–PCR analysis with locked nucleic acid (LNA) primers (27). In the T65 anther, increased expression of *mtRPL27a* or *mtRPL27b* of *S27-T65*$^+$ was detected (a similar result is shown in Fig. S4*B*), whereas no PCR product was found using the *S28-T65*^{s} allele-specific primers (Fig. 3*J*). When we used anthers from *S28* semisterile plants, the expression of *S28-glum*$^+$ was observed in a pattern similar to *S27-T65*$^+$, but again, no PCR product for *S28-T65*^{s} was detected (Fig. 3*K*). To confirm the expression of *mtRPL27* in pollen grains, we analyzed

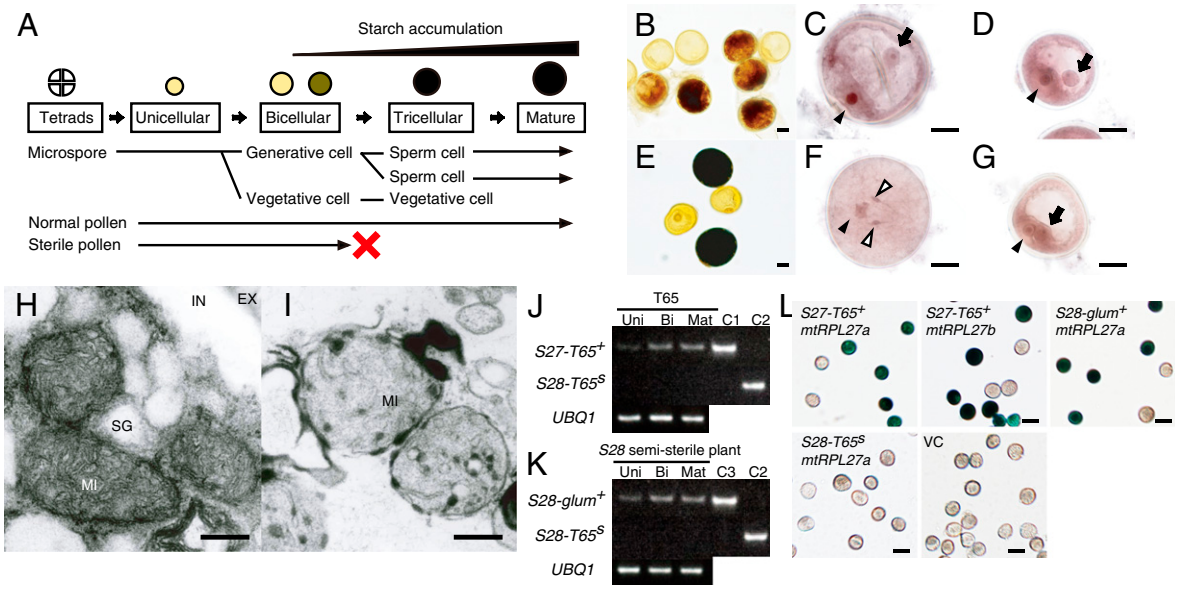

Fig. 3. Mechanism of pollen sterility. (*A*) Schematic of postmeiotic pollen development. (*B–G*) Light-microscopic observation of the pollen phenotype in bicellular (*B–D*) and mature (*E–G*) stages in terms of starch accumulation (*B* and *E*) and nuclei (*C*, *D*, *F*, and *G*). (*C*, *D*, *F*, and *G*) Normal (*C* and *F*) and abnormal (*D* and *G*) pollen grains. Nuclei of vegetative cells, generative cells, and sperm cells are indicated by black arrowheads, black arrows, and white arrowheads, respectively. Scale bars: 10 μm. (*H* and *I*) The ultrastructure of normal (*H*) and abnormal (*I*) pollen grains. MI, mitochondria; EX, exine; IN, intine; SG, starch grain. Scale bars: 0.2 μm. (*J* and *K*) Allele-specific semiquantitative RT–PCR of each *mtRPL27* allele in anthers during the unicellular (Uni), bicellular (Bi), and mature pollen stages (Mat) in T65 (*J*) and in the *S28* semisterile plants (*K*). C1, C2, and C3 indicate the plasmid DNA carrying *mtRPL27* of the *S27-T65*$^+$, *S28-T65*^{s}, and *S27-glum*$^+$ alleles as controls, respectively. (*L*) Analysis of GUS activity under the control of promoters of each *mtRPL27* gene in pollen. VC indicates the control. Scale bars: 50 μm.

the β-glucuronidase (GUS) activity under the control of the promoters of *S27-T65*$^+$ *mtRPL27a*, *S27-T65*$^+$ *mtRPL27b*, *S28-T65*^{s} *mtRPL27a*, and *S28-glum*$^+$ *mtRPL27a* (Fig. 3*L*). GUS activity was observed under the control of the promoters of the three fertile alleles ($^+$), but not *S28-T65*^{s} (Fig. 3*L*). All these results clearly demonstrate that *S28-T65*^{s} contains a loss-of-function allele of *mtRPL27a* with failure of expression.

Origin and Distribution of the *S27-glum*^{s} Allele During AA Genome Divergence. On the basis of a comparison of genomic sequences, Ueda et al. (24) postulated that the duplicated segment on chromosome 8 (*i.e.*, *S27*) was derived from chromosome 4 (*i.e.*, *S28*). We investigated the distribution of the *S27-glum*^{s} alleles among rice AA genome species using two PCR markers, *S27D* and *S27ND*, which determine the presence or absence of the duplicated segment at *S27* (Fig. S5). Among the 172 accessions of the eight AA genome species, the accessions carrying the duplicated segment at *S27* (*S27-T65*$^+$ allele) were widely distributed in all seven species, except for *O. glumaepatula* (Table 1, Fig. S6). This indicates that the segmental genomic duplication carrying *mtRPL27* at *S27* occurred before the divergence of the rice AA genome species and that the duplicated segments at *S27* spread in each species, except *O. glumaepatula*, which is the sole South American species possessing the AA genome and is thought to have an African origin (29). Indeed, the *O. glumaepatula* accessions used in this study were closely related to the *O. barthii* and *O. glaberrima* complex (28, 30, 31) (also see Fig. S6). This evidence led us to hypothesize that the ancestral population of *O. glumaepatula* and *O. barthii* contained both duplicated and nonduplicated genomes at *S27*, and a population with a nonduplicated genome dispersed from Africa to South America and evolved into *O. glumaepatula* in the Amazon basin. In other words, the frequency of the *S27-glum*^{s} allele might have been more prominent in *O. glumaepatula* due to the founder effect, which is a special case of random genetic drift in a population derived from a small number of individuals geographically isolated from the ancestral population. In population genetics, the frequency of genes, including neutral genes of duplicated loci, sometimes changes rapidly through a random sampling effect in a small founder population. These data suggest that geographical isolation played a central role in establishing reproductive isolation between the divergent species despite the selectively neutral allele.

Discussion

Reproductive barriers are thought to play an important role in plant speciation, as in animal speciation (10, 32). The analysis of morphometric data from more than 200 plant genera revealed significant relationships between species and postmating repro-

Table 1. Distribution of the duplicated segment at *S27* among rice AA genome species

	No. of accessions		
	Duplicated segment at *S27*		
Species*	Present	Absent	Total
O. sativa ssp. *japonica* group	31	0	31
O. sativa ssp. *indica* group	70	0	70
O. rufipogon group	23	0	23
O. nivara group	12	0	12
O. glaberrima group	8	0	8
O. barthii group	5	3	8
O. glumaepatula group	0	7	7
O. longistaminata group	1	1	2
O. meridionalis group	11	0	11

*The classification of the accessions into the species groups was based on restriction fragment length polymorphism (28). Detailed data are described in Fig. S6.

GENETICS

ductive barriers, especially postzygotic barriers (10, 32). Therefore, a study on the mechanism of postzygotic barriers is essential to understanding the mechanism of plant species diversification. A large fraction of plant genomes consists of duplicated loci due to the frequent occurrence of segmental genome duplication or polyploidization (33, 34), which has led various authors to propose that the loss-of-function allele of duplicated genes maintained in the genome is a potential source of postzygotic isolation (35, 36). However, only one example of this was reported very recently in an intraspecific hybrid within *A. thaliana* (13). Our study provides experimental evidence that the duplication and subsequent reciprocal loss of the gene, which is expressed and essential for the male gametophyte, also play an important role in hybrid sterility in the F_1 generation.

Materials and Methods

Plant Materials. The Asian cultivated rice T65 (*O. sativa* L. ssp. *japonica* cv. Taichung 65) was crossed with pollen of the South American wild rice species *O. glumaepatula* Steud. (accession: IRGC105668, Brazil) to produce F_1 plants with T65 cytoplasm. Three NILs were developed by continuous backcrossing with T65 and screened at the BC_4 F_1 generation: NIL10 (*S27* heterozygous and *S28-T65* homozygous), NIL22 (*S28* heterozygous and *S27-glum* homozygous), and NIL113 (both *S27* and *S28* heterozygous). The genotypes of each NIL across the entire genomic region were determined using restriction fragment length polymorphism markers. The progeny of NIL10 and NIL22 were used for high-resolution mapping of *S27* and *S28*, respectively. To analyze the epistatic interaction, the progeny of NIL113 were used.

Evaluation of Pollen Fertility. Panicles at the flowering stage were fixed and stored in 70% (wt/wt) ethanol. Six anthers from one spikelet collected just before flowering were squashed on a glass slide in 1% (wt/vol) iodine-potassium iodide (I_2–KI) solution. More than 200 pollen grains were evaluated for pollen fertility under an Axioplan light microscope (Zeiss). Pollen grains that were morphologically the same as grains of T65 were scored as normal. Aborted, unstained, and small grains were scored as sterile.

Map-Based Cloning. For the high-resolution mapping of *S27* and *S28*, we used simple sequence repeat, cleaved amplified polymorphic sequence, and single nucleotide polymorphism markers (Table S2). Genomic DNA fragments containing the candidate genes were cloned in the Ti-plasmid binary vector pPZP2H-lac (37). Using *Agrobacterium*-mediated transformation (38), these genomic fragments were introduced into the pollen-semisterile plants with the genotype *S27-T65*$^+$/*S27-glum*^{s}|*S28-T65*^{s}/*S28-T65*^{s} and into the other pollen-semisterile plants with the genotype *S27-glum*^{s}|*S27-glum*^{s}/*S28-T65*^{s}/*S28-glum*$^+$.

Observation of Pollen Development. Panicles in the meiotic-to-mature stages were collected continuously to monitor pollen development from the unicellular-to-mature stage. Panicles were placed in fixative solution containing 4% (wt/vol) paraformaldehyde, 0.25% (wt/vol) glutaraldehyde, 0.02% (vol/vol) Triton X-100, and 100 mM sodium phosphate (pH 7.5) for 24 h at 4°C and then rinsed in 100 mM sodium phosphate buffer. The hematoxylin staining procedure used followed that of Chang and Neuffer (39) with minor modifications.

Ultrastructural Analysis. Anthers at the mature stage were vacuum-infiltrated three times for 10 min with fixative (4% paraformaldehyde and 1% glutaraldehyde in 0.05 M cacodylate buffer, pH 7.4). The procedures for the ultrastructural studies were essentially the same as those described by Hara-Nishimura et al. (40).

Expression Analysis. Total RNA was extracted using the RNeasy plant kit (Qiagen). The sequences of the primer pairs were 5′-CCG TGA CTC TAA CCC TAA G-3′ and 5′-ATG GAA GCG GGT TCC TCT T-3′ for *mtRPL27* and 5′-CTG TCA ACT GCC GCA AGA AG-3′ and 5′-GGC GAG TGA CGC TCT AGT TC-3′ for *UBQ1* (*Os03g0234200*). Following Itoh et al. (41), we sampled 1–2 mm of the anthers at the unicellular stage, 2 mm of the anthers at the bicellular stage, and the anthers at the mature stage. First-strand cDNA was synthesized from ~1 μg of total RNA with an oligo(dT) primer and the OmniScript RT kit (Qiagen). Expression of *mtRPL27* at the various stages was quantified with real-time PCR analysis using 10% of the resulting cDNA as template. Real-time PCR was performed with the LightCycler system (Roche) and a QuantiTect SYBR Green PCR kit (Qiagen). For this analysis, a linear standard curve and threshold cycle number versus log (designated transcript level) were constructed using a series of dilutions of each PCR product (10^{-17}, 10^{-18}, 10^{-19}, and 10^{-20} M); the transcript levels in all unknown samples were determined using the standard curve. We used *UBQ1* as an internal standard for normalizing the cDNA concentrations. Data represent the average of three replicates of the first-strand cDNA. Allele-specific semiquantitative RT–PCR was performed using LNA primers (27). The primer sequences are listed in Table S3. The PCR was conducted using AmpliTaq Gold DNA polymerase (Applied Biosystems) and consisted of a 5-min Taq activation step followed by 33 cycles at 94°C for 30 s, 68.4°C for 20 s, and 72°C for 20 s.

Promoter GUS Assay. To analyze the GUS activity in the pollen, the promoter sequence for each *mtRPL27* gene was digested using the appropriate restriction enzyme or amplified with PCR using a genomic clone as the template. When PCR was used to clone the promoter sequence, the resulting product was cloned into pCRII (Invitrogen) and was sequenced to confirm that no base substitution had occurred during PCR. The promoter sequences were introduced at the front of the GUS reporter gene of pBI-Hm (42) to produce a fusion with the GUS reporter gene. The constructs were introduced using *Agrobacterium*-mediated transformation (38) into T65. The regenerated plants containing only one copy of the insert were screened by Southern blot analysis using a GUS DNA fragment as the probe. Pollen of regenerated plants was sampled, and the GUS activity was analyzed as described previously by Matsuoka and Sanada (43).

Distribution Analysis. The presence and absence of the duplicated segment at *S27* was investigated in the AA genome rice species with the markers *S27D* and *S27ND*, respectively, using KOD plus DNA polymerase (TOYOBO). The primer pair used for the *S27D* marker was 5′-TTG AAT TCC GAG AGT CTG GC-3′ and 5′-GGT CGT CGG AGT GGT AGA CGA AG-3′ and that used for the *S27ND* marker was 5′-GGT CGT CGG AGT GGT AGA CGA AG-3′ and 5′-TGT TCA CCA AAT GAC TCC AAA TCG-3′. The PCR comprised an initial denaturation at 96°C for 2 min, followed by 30 cycles at 96°C for 35 s, 60°C for 30 s, and 68°C for 2 min.

ACKNOWLEDGMENTS. This work was supported by grants from the Ministry of Agriculture, Forestry, and Fisheries of Japan (Integrated Research Project for Plants, Insects, and Animals Using Genome Technology GD-2003 to A. Y, and K. D., and Genomics for Agricultural Innovation QTL-5002 to A.Y. and IPG-0015 to K.D.) and a Grant-in-Aid from the Ministry of Education, Culture, Sports, Science, and Technology of Japan (18075006 to M.M.)

1. Darwin C (1859) *On the Origin of Species by Means of Natural Selection, or the Preservation of Favoured Races in the Struggle for Life* (J. Murray, London).
2. Coyne JA, Orr HA (2004) *Speciation* (Sinauer Associates, Sunderland, MA).
3. Dobzhansky T (1937) *Genetics and the Origin of Species* (Columbia University Press, New York).
4. Barbash DA, Siino DF, Tarone AM, Roote J (2003) A rapidly evolving MYB-related protein causes species isolation in *Drosophila*. *Proc Natl Acad Sci USA* 100:5302–5307.
5. Brideau NJ, et al. (2006) Two Dobzhansky-Muller genes interact to cause hybrid lethality in *Drosophila*. *Science* 314:1292–1295.
6. Presgraves DC, Balagopalan L, Abmayr SM, Orr HA (2003) Adaptive evolution drives divergence of a hybrid inviability gene between two species of *Drosophila*. *Nature* 423:715–719.
7. Tang S, Presgraves DC (2009) Evolution of the *Drosophila* nuclear pore complex results in multiple hybrid incompatibilities. *Science* 323:779–782.
8. Masly JP, Jones CD, Noor MAF, Locke J, Orr HA (2006) Gene transposition as a cause of hybrid sterility in *Drosophila*. *Science* 313:1448–1450.
9. Stebbins GL (1958) The inviability, weakness, and sterility of interspecific hybrids. *Adv Genet* 9:147–215.
10. Rieseberg LH, Willis JH (2007) Plant speciation. *Science* 317:910–914.
11. Bomblies K, Weigel D (2007) Hybrid necrosis: autoimmunity as a potential gene-flow barrier in plant species. *Nat Rev Genet* 8:382–393.
12. Bomblies K, et al. (2007) Autoimmune response as a mechanism for a Dobzhansky-Muller-type incompatibility syndrome in plants. *PLoS Biol* 5:e236.
13. Bikard D, et al. (2009) Divergent evolution of duplicate genes leads to genetic incompatibilities within *A. thaliana*. *Science* 323:623–626.
14. Long Y, et al. (2008) Hybrid male sterility in rice controlled by interaction between divergent alleles of two adjacent genes. *Proc Natl Acad Sci USA* 105:18871–18876.
15. Chu YE, Morishima H, Oka HI (1969) Reproductive barriers distributed in cultivated rice species and their wild relatives. *Jpn J Genet* 44:207–223.
16. Oka HI (1998) *Origin of Cultivated Rice* (JSSP/Elsevier, Tokyo).
17. Chen J, et al. (2008) A triallelic system of *S5* is a major regulator of the reproductive barrier and compatibility of indica-japonica hybrids in rice. *Proc Natl Acad Sci USA* 105:11436–11441.
18. Oka HI (1974) Analysis of genes controlling F_1 sterility in rice by the use of isogenic lines. *Genetics* 77:521–534.

19. Akimoto M, Shimamoto Y, Morishima H (1998) Population genetic structure of wild rice *Oryza glumaepatula* distributed in the Amazon flood area influenced by its life-history traits. *Mol Ecol* 7:1371–1381.
20. Sobrizal, Matsuzaki Y, Sanchez PL, Ikeda K, Yoshimura A (2000) Identification of a gene for male gamete abortion in backcross progeny of *Oryza sativa* and *Oryza glumaepatula*. *Rice Genet Newsl* 17:59–61.
21. Sobrizal, Matsuzaki Y, Sanchez PL, Ikeda K, Yoshimura A (2000) Mapping of F_1 pollen semi-sterility gene found in backcross progeny of *Oryza sativa* L. and *Oryza glumaepatula* Steud. *Rice Genet Newsl* 17:61–63.
22. Sobrizal, Matsuzaki Y, Yoshimura A (2001) Mapping of a gene for pollen semi-sterility on chromosome 8 of rice. *Rice Genet Newsl* 18:59–61.
23. Sobrizal, Matsuzaki Y, Yoshimura A (2002) Mapping of pollen semi-sterility gene, *S28* (t), on rice chromosome 4. *Rice Genet Newsl* 19:80–82.
24. Ueda M, et al. (2006) Promoter shuffling at a nuclear gene for mitochondrial RPL27. Involvement of interchromosome and subsequent intrachromosome recombinations. *Plant Physiol* 141:702–710.
25. Sakata K, et al. (2002) RiceGAAS: An automated annotation system and database for rice genome sequence. *Nucleic Acids Res* 30:98–102.
26. Wower IK, Wower J, Zimmermann RA (1998) Ribosomal protein L27 participates in both 50 S subunit assembly and the peptidyl transferase reaction. *J Biol Chem* 273: 19847–19852.
27. Latorra D, Arar K (2003) Design considerations and effects of LNA in PCR primers. *Mol Cell Probes* 17:253–259.
28. Doi K, Nonomura MN, Yoshimura A, Iwata N, Vaughan DA (2000) RFLP relationships of A-genome species in the genus *Oryza*. *J. Fac. Agr. Kyushu Univ.* 45:83–98.
29. Vaughan DA, Kadowaki K, Kaga A, Tomooka N (2005) On the phylogeny and biogeography of the genus *Oryza*. *Breed Sci* 55:113–122.
30. Wang ZY, Second G, Tanksley SD (1992) Polymorphism and phylogenetic relationships among species in the genus *Oryza* as determined by analysis of nuclear RFLPs. *Theor Appl Genet* 83:565–581.
31. Cheng CY, Tsuchimoto S, Ohtsubo H, Ohtsubo E (2002) Evolutionary relationships among rice species with AA genome based on SINE insertion analysis. *Genes Genet Syst* 77:323–334.
32. Rieseberg LH, Wood TE, Baack EJ (2006) The nature of plant species. *Nature* 440: 524–527.
33. Bowers JE, Chapman BA, Rong J, Paterson AH (2003) Unravelling angiosperm genome evolution by phylogenetic analysis of chromosomal duplication events. *Nature* 422: 433–438.
34. Moore RC, Purugganan MD (2005) The evolutionary dynamics of plant duplicate genes. *Curr Opin Plant Biol* 8:122–128.
35. Werth CR, Windham MD (1991) A model for divergent, allopatric speciation of polyploid pteridophytes resulting from silencing of duplicate-gene expression. *Am Nat* 137:515–526.
36. Lynch M, Conery JS (2000) The evolutionary fate and consequences of duplicate genes. *Science* 290:1151–1155.
37. Fuse T, Sasaki T, Yano M (2001) Ti-plasmid vectors useful for functional analysis of rice genes. *Plant Biotechnol* 18:219–222.
38. Hiei Y, Ohta S, Komari T, Kumashiro T (1994) Efficient transformation of rice (*Oryza sativa* L.) mediated by *Agrobacterium* and sequence analysis of the boundaries of the T-DNA. *Plant J* 6:271–282.
39. Chang MT, Neuffer MG (1989) Maize microsporogenesis. *Genome* 32:232–244.
40. Hara-Nishimura I, Takeuchi Y, Nishimura M (1993) Molecular characterization of a vacuolar processing enzyme related to a putative cysteine proteinase of *Schistosoma mansoni*. *Plant Cell* 5:1651–1659.
41. Itoh J, et al. (2005) Rice plant development: From zygote to spikelet. *Plant Cell Physiol* 46:23–47.
42. Nomura M, et al. (2000) The promoter of *rbcS* in a C3 plant (rice) directs organ-specific, light-dependent expression in a C4 plant (maize), but does not confer bundle sheath cell-specific expression. *Plant Mol Biol* 44:99–106.
43. Matsuoka M, Sanada Y (1991) Expression of photosynthetic genes from the C_4 plant, maize, in tobacco. *Mol Gen Genet* 225:411–419.